# EPLIN mediates linkage of the cadherin–catenin complex to F-actin and stabilizes the circumferential actin belt

**Kentaro Abe and Masatoshi Takeichi***

RIKEN Center for Developmental Biology, 2-2-3 Minatojima-Minamimachi, Chuo-ku, Kobe 650-0047, Japan

This contribution is part of the special series of Inaugural Articles by members of the National Academy of Sciences elected on May 1, 2007.

Contributed by Masatoshi Takeichi, November 5, 2007 (sent for review September 4, 2007)

**The cadherin–catenin complex is the major machinery for cell–cell adhesion in many animal species. This complex in general associates with actin fibers at its cytoplasmic side, organizing the adherens junction (AJ). In epithelial cells, the AJ encircles the cells near their apical surface and forms the ''zonula adherens'' or ''adhesion belt.'' The mechanism as to how the cadherin–catenin complex and F-actin cooperate to generate these junctional structures, however, remains unknown. Here, we show that EPLIN (epithelial protein lost in neoplasm; also known as Lima-1), an actin-binding protein, couples with α-catenin and, in turn, links the cadherin–catenin complex to F-actin. Without EPLIN, this linkage was unable to form. When EPLIN had been depleted in epithelial cells, the adhesion belt was disorganized and converted into zipper-like junctions in which actin fibers were radially arranged. However, nonjunctional actin fibers were not particularly affected by EPLIN depletion. As EPLIN is known to have the ability to suppress actin depolymerization, our results suggest that EPLIN functions to link the cadherin–catenin complex to F-actin and simultaneously stabilizes this population of actin fibers, resulting in the establishment of the adhesion belt.**

adherens junction | epithelial cells | cell adhesion

Epithelial cells are characterized by their apical–basal polarity. Near the apical surface of the cells, a class of cell–cell junction structures, the adherens junction (AJ), develops (1). The AJ encircles the cells, together with a bundle of cortical actin filaments, organizing the ''zonula adherens'' or ''adhesion belt.'' This actin bundle, called the circumferential actin belt, is known to play a number of roles in epithelial morphogenesis (2, 3): For example, the contractility of this belt contributes to the constriction of the apical end of epithelial cells (4–6) and the rearrangement of cells undergoing convergent extension (7, 8). Small Rho GTPases control the tension of these actin fibers and regulate the shape of epithelial cells (9).

The AJ comprises cadherin, catenins, and other associated proteins (1). Cadherins interact homophilically via their extracellular domain, functioning as a physical linker between the confronting cell membranes. The cytoplasmic region of cadherin binds β-catenin; and this catenin, in turn, associates with α-catenin. α-Catenin is indispensable for cadherin-mediated cell adhesions (10, 11). In the absence of α-catenin, the AJ is disrupted, and the apical actin belt becomes segregated from the cadherin–catenin complex (12). In cadherin-deficient cells, such as L cells, re-expression of not only the full-length cadherins but also cadherin–α-catenin fusion proteins can restore their normal cadherin-mediated adhesiveness; whereas cadherin mutants, which are unable to bind α-catenin, cannot do so (13). Biochemical studies showed that α-catenin can interact with actin filaments (14), and the cadherin–α-catenin fusion constructs and wild-type cadherins were shown to be tethered to the cytoskeleton (15, 16). Cytochemically, the cadherin–catenin complex colocalizes with actin filaments in various ways. In epithelial apical junctions, the complex associates with the circumferential actin belt, whereas it attaches to radial actin fibers in nonepithelial cells (17) or in early phases of epithelial cell–cell contacts (18). In certain cell types, cadherins become anchored at actin fibers undergoing ''retrograde flow'' in a α-catenin-dependent manner (19).

Through these and other observations, it has been believed that the cadherin–catenin complex is physically linked with actin fibers via α-catenin and that this linkage is crucial for the maintenance of the AJ. This model was, however, challenged by the recent finding that the reconstructed cadherin–catenin complex was unable to directly bind actin filaments *in vitro* (20, 21). These observations, however, could be reconciled by assuming a number of possible mechanisms, including one by which unidentified mediators might serve as a bridge between the cadherin-bound α-catenin and F-actin (22). In the present study, we identified EPLIN (epithelial protein lost in neoplasm; also known as Lima-1) as a novel α-catenin partner. EPLIN is known to be an actin-binding protein, which enhances bundling of actin filaments and stabilizes them by suppressing F-actin depolymerization (23). Using epithelial cell lines, we found that EPLIN mediated the interaction of the cadherin–catenin complex with F-actin at the apical cell–cell junctions. Depletion of EPLIN disrupted not only the apical actin assembly but also the adhesion belt. We also could reconstitute a stable interaction between the cadherin–catenin-EPLIN complex and F-actin *in vitro*. These observations demonstrate EPLIN to be a key molecule linking the cadherin–catenin complex to F-actin, and stabilizing the adhesion belt.

## Results

**EPLIN Interacts with α-Catenin and Forms a Cadherin–Catenin–EPLIN Complex.** By analyzing immunoprecipitates collected with anti-αE-catenin (abbreviated as α-catenin) antibodies from mouse tissue lysates, we screened for novel proteins interacting with α-catenin. Peptide MS/MS analysis identified one of the precipitated materials as EPLIN, an actin-binding molecule (24, 25). Further immunoprecipitation experiments showed that EPLIN was coprecipitated not only with α-catenin but also with E-cadherin (Fig. 1*A*) or β-catenin (data not shown) from lysates of DLD-1 cells, a polarized epithelial cell line derived from human colon carcinoma (26), suggesting that EPLIN may associate with the entire cadherin–catenin complex. EPLIN has two isoforms,

Author contributions: K.A. designed research; K.A. performed research; K.A. and M.T. analyzed data; and K.A. and M.T. wrote the paper.

The authors declare no conflict of interest.

Freely available online through the PNAS open access option.

*To whom correspondence should be addressed. E-mail: takeichi@cdb.riken.jp.

This article contains supporting information online at www.pnas.org/cgi/content/full/0710504105/DC1.

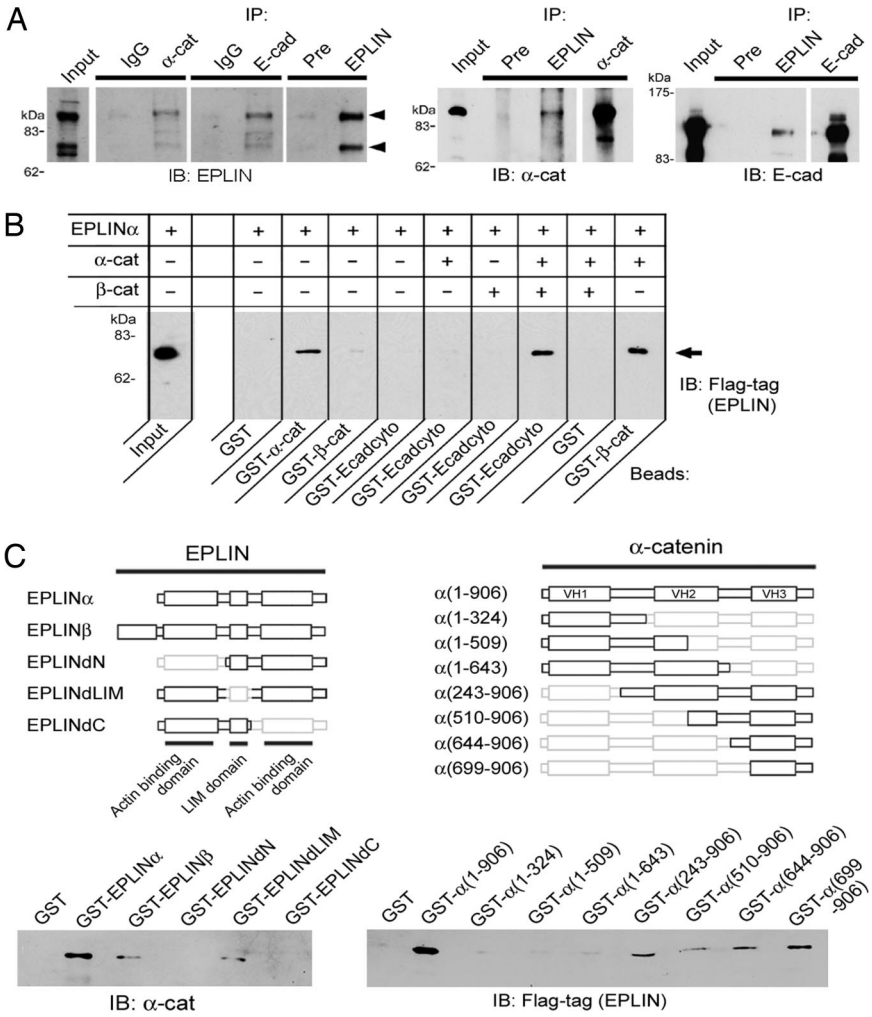


**Fig. 1.** EPLIN interacts with α-catenin to couple to the cadherin–β-catenin complex. (*A*) Lysates of DLD-1 cells were subjected to immunoprecipitation (IP) with antibodies against α-catenin (α-cat), E-cadherin (E-cad), or EPLIN. As a control, preimmune serum (Pre), or mouse or rabbit anti-GFP IgGs (IgG) were used. The precipitates were analyzed by SDS/PAGE and Western blotting to detect α-cat, E-cad, or EPLIN. Arrowheads indicate the α (*Lower*) and β (*Upper*) isoforms of EPLIN. In Input, 2% of the lysate used for immunoprecipitation was loaded in each experiment. IB, immunoblot. (*B*) *In vitro* binding between purified proteins. Recombinant EPLINα-Flag proteins, from which the GST tag had been removed (SI Fig. 7), were incubated with various GST-fusion protein-coated beads, as indicated. The arrow points to the pulled-down EPLIN, detected by Western blotting with antibodies against Flag tag. EPLIN efficiently coprecipitates with GST-α-cat, but not with GST, GST-β-cat (β-catenin), or GST-Ecadcyto. In the presence of both α-catenin and β-catenin (GST tag removed), however, EPLIN can be pulled down by GST-Ecadcyto. (*C*) *In vitro* binding between purified fragments of α-catenin and EPLINα-Flag, carrying deletions of each protein. The diagrams show the deletion series of EPLIN (*Left*) and α-catenin (*Right*) (see also SI Fig. 7). A GST tag was fused to the N terminus of each molecule. The interaction of the proteins was analyzed by Western blotting with antibodies against Flag tag (for EPLIN) or α-catenin. All constructs having the VH3 domain bound EPLIN. A faint interaction of α (amino acids 1–643) with EPLIN was detectable, but it was not reproducible.

EPLINα and EPLINβ (25), and both isoforms were found in the precipitates. To determine which elements in the cadherin–catenin complex directly bound EPLIN, we analyzed interactions between their recombinant proteins (Fig. 1*B*), and found that recombinant EPLIN could be pulled down by GST-α-catenin, but not by GST-β-catenin or GST-E-cadherin cytoplasmic domain (GST-Ecadcyto), indicating that EPLIN interacted solely with α-catenin. However, when α-catenin was added to the reaction mixture, EPLIN could be coprecipitated with GST-β-catenin, but not with GST-Ecadcyto; further, in the presence of both α-catenin and β-catenin, EPLIN coprecipitated with GST-Ecadcyto. These results suggest that EPLIN associated with the cadherin–β-catenin–α-catenin complex via α-catenin.

To define which domains of EPLIN and α-catenin were necessary for their interactions, we constructed a series of their deletion mutants as GST fusions and then analyzed their ability to interact with one another (Fig. 1*C*). Both EPLINα and EPLINβ isoforms were found to bind to α-catenin. EPLIN has a central LIM domain and N- and C-terminal domains involved in actin binding. Deletion of the LIM domain had no effect on the EPLIN–α-catenin interaction. However, removal of either the N- or C-terminal region abrogated it, suggesting that EPLIN required both of these regions to interact with α-catenin. α-Catenin has three domains, VH (vinculin homology) 1–3, each of which is known to bind specific proteins; for example, VH1 to β-catenin, VH2 to formin-1 and vinculin, and VH3 (together with the adjacent C-terminal region) to ZO-1 and actin (14, 27, 28). Deletion analysis revealed that only the constructs having the VH3 plus C-terminal region (VH3-C region) or the VH3-C region itself could bind EPLIN (Fig. 1*C*), suggesting that this portion of α-catenin was essential for the interaction with EPLIN.

**EPLIN Localizes at Cell–Cell Junction in a α-Catenin-Dependent Manner.** Subcellular localization of EPLIN was analyzed in two epithelial cell lines, DLD-1 and MDCK. In these cell lines,

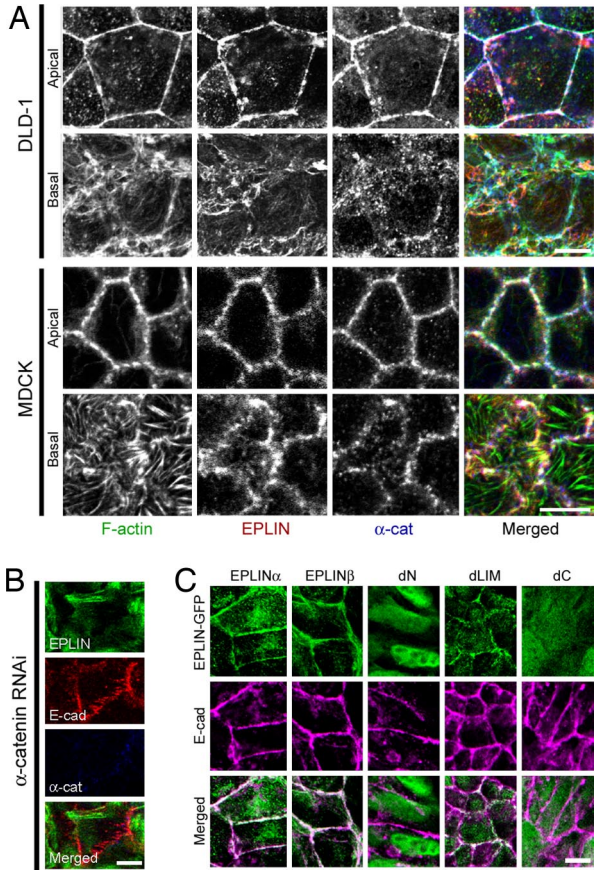


**Fig. 2.** EPLIN localization at cell–cell junctions requires α-catenin. (*A*) Distribution of EPLIN, α-catenin, and F-actin, which are triple-stained, in DLD-1 or MDCK cells. Confocal sections focused around the apical-most and basal-most portions of the cells are shown. These three proteins colocalize well in the apical level, but not in the basal level, of the cells. In particular, EPLIN is not detectable along actin stress fibers in MDCK cells. The distributions of E-cadherin and α-catenin are essentially identical; therefore, only the data for either one of them are shown. (*B*) DLD-1 cells transfected with siRNA against α-catenin do not show the colocalization of E-cadherin and EPLIN. Depletion of α-catenin was confirmed by Western blot analysis (SI Fig. 8). (*C*) DLD-1 cells stably transfected with various EPLIN constructs shown in Fig. 1*C*. EPLINα, EPLINβ, and EPLINdLIM show cell junctional accumulation, but EPLINdN and EPLINdC do not. (Scale bars: 10 μm.)

E-cadherin and catenins are distributed along the lateral cell–cell contact sites; and at the apical-most portion of the cells, they colocalize with thin actin filaments, constituting the adhesion belt. Immunostaining for EPLIN detected this protein as fine signals localized along the adhesion belt, together with cadherin and catenins and F-actin (Fig. 2*A*). Some of the colocalized signals of EPLIN and E-cadherin or catenins appeared to extend down toward the basal portions of the cell junction in both cell lines. However, in DLD-1 cells, the epithelial morphology of cell–cell contacts was distorted at the basal-most level, as represented by irregular distributions of F-actin and α-catenin (or E-cadherin). In these regions, EPLIN overlapped with F-actin, but their distributions were not identical. In the case of MDCK cells, nonjunctional stress fibers were present at the basal level, and EPLIN was hardly detectable along these stress fibers. These observations suggest that EPLIN has a preference to colocalize with the cell junctional population of F-actin. Similar codistributions of EPLIN with F-actin and the cadherin–catenin complex were also observed in other epithelial cell lines.

The above *in vitro* binding assays showed that the interaction between EPLIN and the cadherin cytoplasmic domain required α-catenin (Fig. 1*B*). To test whether this is also the case in cells, we knocked down α-catenin expression in DLD-1 cells by using siRNA. As reported (12), when α-catenin had been depleted, E-cadherin accumulated only irregularly at cell–cell contact sites, and the cells lost their adhesion belt structures. In these cells, the colocalization of EPLIN and E-cadherin was abrogated (Fig. 2*B*), and also the amount of EPLIN coimmunoprecipitated with E-cadherin became only residual [supporting information (SI) Fig. 6]. We also generated DLD-1 lines stably expressing exogenous EPLINα or EPLINβ and deletion constructs of EPLINα (Fig. 2*C*). The full-length EPLINα or EPLINβ was recruited to cell–cell junctions, as expected. Deletion of the central LIM domain had no effect on the junctional localization of EPLINα, whereas N- or C terminus-deleted EPLINα, which were unable to bind α-catenin, were not localized to E-cadherin-mediated cell junctions. All of these results confirmed that the binding of EPLIN to α-catenin was essential for the former to interact with cadherin and localize at cell–cell contacts.

**EPLIN Is Indispensable for Apical Actin Belt Formation.** We next examined the role of EPLIN in DLD-1 cell junctions by knocking down EPLIN expression with siRNA against human EPLIN. EPLIN depletion had dramatic effects on cell junctions: The honeycomb-like organization of the adhesion belts delineated by E-cadherin or F-actin was completely lost; instead, E-cadherin exhibited only a punctate accumulation at cell–cell contact zones (Fig. 3*A*). Intriguingly, in these cells, actin fibers became radially organized, terminating at the E-cadherin puncta, the morphological profile of which was reminiscent of the zipper-like junction seen in the early phases of cell–cell contacts between keratinocytes (18, 29) or in fibroblasts (17). Control RNAi had no such effects. Basal, nonjunctional actin fiber organization appeared to have not particularly been affected by EPLIN RNAi; however, we could not exclude the possibility that a subtle reorganization of actin fibers might have been induced.

To check the specificity of the siRNA effects, we transfected DLD-1 cells with mouse EPLIN cDNA, and subsequently treated the transfectants with human EPLIN siRNA. Cells expressing mouse EPLIN did not respond to the human EPLIN depletion (Fig. 3*B*), ensuring that the above RNAi effects were an EPLIN-specific phenomenon. These observations suggest that EPLIN was essential for organization of epithelial apical junctions; for without it, the adhesion belts were transformed into premature or fibroblast-type junctions.

**EPLIN Stabilizes Apical Actin Bundles via the Connection with the Cadherin–Catenin Complex.** EPLIN has the ability to stabilize actin filaments by suppressing their depolymerization (23). As a test for whether the actin-stabilizing activity of EPLIN was involved in the above observations, we treated DLD-1 cells, transfected with control or EPLIN siRNA, with 1 μM latrunculin A, an actin polymerization inhibitor, for 30 min. After this treatment, apical junctional actin became puctated, but maintained its association with EPLIN and α-catenin (Fig. 4*A*) or E-cadherin (data not shown). These actin puncta did not show further degradation during prolonged incubation with latrunculin at least for 2 h, suggesting that this fraction of actin was stable. However, when EPLIN-depleted DLD-1 cells had been treated with latrunculin, no actin signals colocalizing with cadherin or α-catenin were detectable (Fig. 4*A*). These results support the notion that EPLIN was important for stabilizing F-actin associated with the cadherin–catenin complex.

To examine whether the ability of EPLIN to stabilize the apical actin belts depended on its association with the cadherin–catenin complex or not, we used R2/7 cells, a α-catenin-deficient line derived from DLD-1 (12). In the R2/7 cells, the adhesion belt is absent; however, in their apical portions, actin bundles often remain as a ZO-1-positive ring-like structure in many of

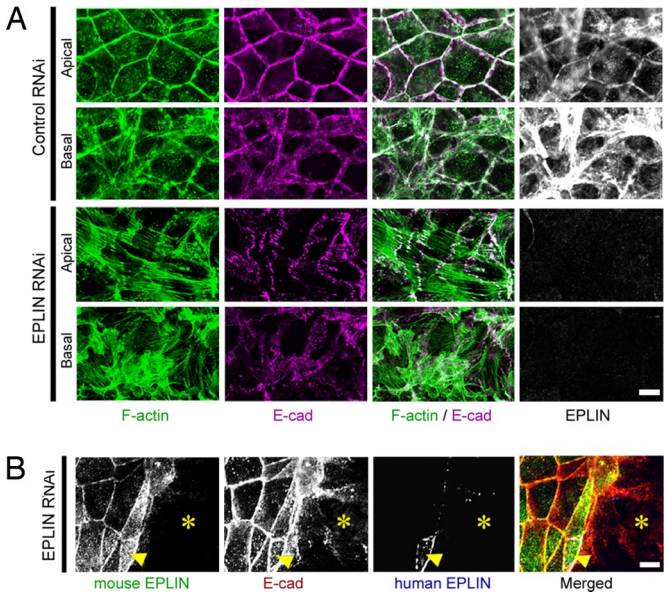


**Fig. 3.** EPLIN is indispensable for adhesion belt formation. (*A*) EPLIN depletion disrupts the apical organization of F-actin. DLD-1 cells transfected with control siRNA or siRNA against EPLIN were triple-stained for F-actin, E-cadherin, and EPLIN. Apical-most and basal-most confocal sections are shown. Note that the circular arrangement of F-actin along the adhesion belt is converted into a radial one by EPLIN depletion, which was confirmed by Western blot analysis (SI Fig. 7). (*B*) Rescue of the EPLIN-depletion phenotypes by mouse EPLIN expression. DLD-1 cells were transfected with mouse EPLIN$\alpha$-GFP cDNA; and then, a mixed culture of cells expressing and not expressing mouse EPLIN was treated with siRNA against human EPLIN. Green, mouse EPLIN; magenta, E-cadherin; blue, human EPLIN. Asterisks indicate a portion of the culture not expressing mouse EPLIN. In this portion, E-cadherin distribution is disorganized; whereas, in the mouse EPLIN-positive area, E-cadherin remains to organize the adhesion belts. The arrow points to a cell that escaped from the siRNA treatment, resulting in expression of both mouse and human EPLIN. The EPLIN antibodies used here recognize only the human EPLIN. (Scale bars: 10 $\mu$m.)

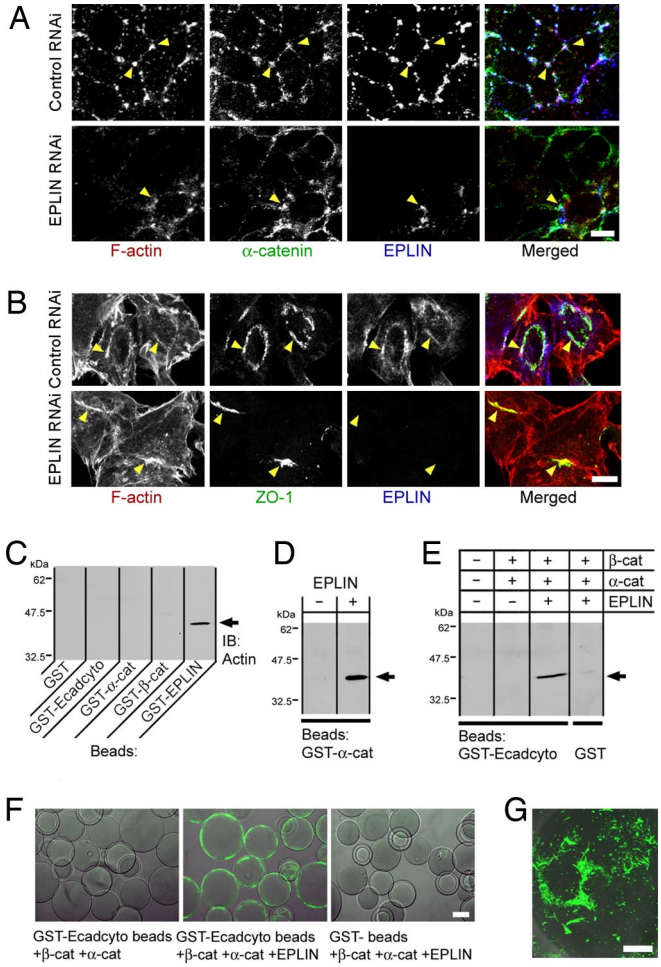


**Fig. 4.** EPLIN stabilizes apical actin bundles and links them to the cadherin–catenin complex. (*A*) EPLIN depletion enhances the latrunculin A sensitivity of F-actin at AJ. DLD-1 cells treated with control or EPLIN siRNA were incubated with 1 $\mu$M latrunculin A for 30 min, then fixed, and triple-stained for F-actin, $\alpha$-catenin, and EPLIN. F-actin remains as clusters in the control cultures, colocalizing with $\alpha$-catenin and EPLIN, as indicated by the arrowheads. When EPLIN is depleted, F-actin and $\alpha$-catenin becomes dispersed. EPLIN expression is not down-regulated in some cells in the EPLIN RNAi cultures, and these cells maintain actin clusters (arrowheads). (*B*) Apical actin bundles in $\alpha$-catenin-deficient cells are sensitive to EPLIN depletion. R2/7 cells were treated with control or EPLIN siRNA, fixed, and triple-stained for F-actin, ZO-1, and EPLIN. Arrowheads in the control show examples of ZO-1-positive F-actin bundles, where EPLIN is also localized. In EPLIN-depleted cells, the ZO-1 positive structures are collapsed, as indicated by the arrowheads. (*C–E*) *In vitro* binding between F-actin and various proteins. GST-fusion protein-coated beads were incubated with 4 $\mu$g of polymerized actin (5–10 $\mu$m long), and collected by centrifugation at 3,500 $\times$ *g*. The precipitates were washed extensively and subjected to Western blot assays for detecting the bound actin (arrows). In *D*, GST-$\alpha$-catenin-coated beads were preincubated with purified EPLIN, washed, and then used for the above assay. In *E*, GST-Ecadcyto-coated beads were sequentially incubated with recombinant $\beta$-catenin, $\alpha$-catenin, and EPLIN, before use for the F-actin pull-down assay. Ecadcyto can interact with actin, but only when $\beta$-catenin, $\alpha$-catenin, and EPLIN are present all together. (*F* and *G*) Beads incubated with F-actin were stained with Alexa Fluor-488-conjugated phalloidin, followed by observations with a confocal fluorescence microscope. In *G*, a higher magnification view of the surface of a GST-Ecadcyto bead incubated with $\beta$-catenin, $\alpha$-catenin, and EPLIN is shown, on which filamentous actins are deposited. (Scale bars: *A*, *B*, and *G*, 10 $\mu$m; *F*, 50 $\mu$m.)

the cells (12), which is assumed to be a remnant structure of the adhesion belt. In these cells, EPLIN was localized along such ZO-1-positive actin rings (Fig. 4*B*). When EPLIN was knocked down, all of these actin rings disappeared, and the originally circular ZO-1 signals appeared collapsed (Fig. 4*B*). These results suggest that EPLIN can stabilize the apical F-actin rings by associating with them even in the absence of $\alpha$-catenin.

Next, we sought to test whether EPLIN served not only as an actin stabilizer but also as a linker between the cadherin–catenin complex and actin filaments. We prepared Sepharose beads coated with GST, GST-Ecadcyto, GST-$\alpha$-catenin, GST-$\beta$-catenin, or GST-EPLIN$\alpha$ and incubated them with polymerized actins to observe whether they could cosediment together. Among the five beads tested, only GST-EPLIN$\alpha$ beads could sediment actin (Fig. 4*C*). Although the soluble GST-$\alpha$-catenin is known to interact with F-actin (14), our GST-$\alpha$-catenin beads could not precipitate any actin, supporting the observation that monomeric $\alpha$-catenin is unable to bind actin fibers (21). However, once the GST-$\alpha$-catenin had been preincubated with EPLIN proteins to induce the formation of $\alpha$-catenin–EPLIN complexes, the beads then became able to precipitate actin (Fig. 4*D*). Moreover, although the cadherin–$\beta$-catenin–$\alpha$-catenin complex beads, prepared by a sequential incubation of the GST-Ecadcyto beads with $\beta$-catenin and $\alpha$-catenin, were unable to precipitate actin, further addition of EPLIN to this complex allowed it to interact with actin (Fig. 4*E*).

EPLIN was shown to interact with both G-actin and F-actin (23). To test whether EPLIN precipitated F-actin onto the beads, we incubated the treated beads with fluorphore-conjugated phalloidin, known to bind only F-actin (30). Fluorescence-microscopic analysis of these beads showed that phalloidin stained the GST-Ecadcyto beads preincubated serially with

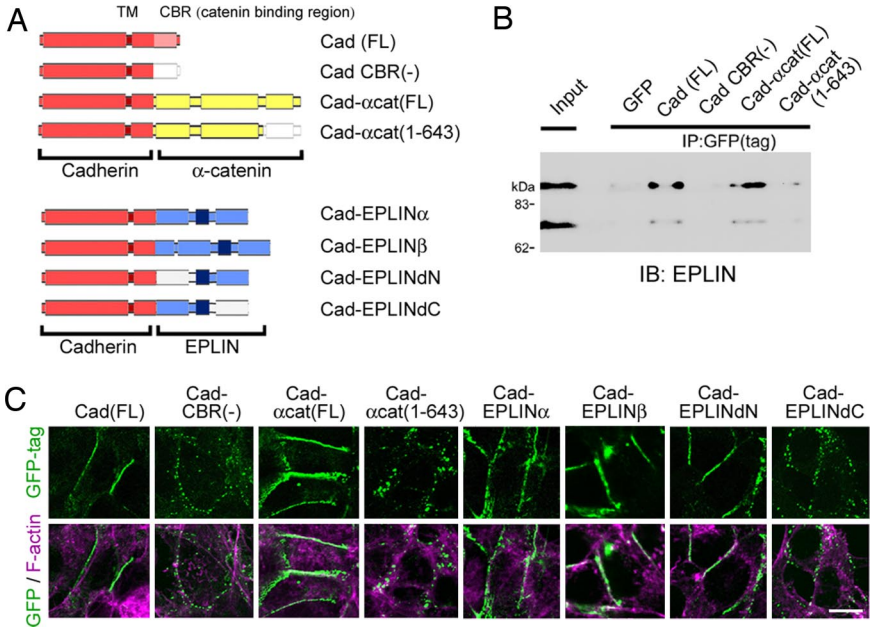


**Fig. 5.** The cadherin–EPLIN association is sufficient to link junctional actin rings to cadherin. (*A*) Diagrams showing fusion constructs between cadherin and α-catenin (*Upper*) (13) or EPLIN (*Lower*). To use these constructs for generating transfectants, a GFP tag was fused to the C terminus of each molecule. (*B*) Binding of EPLIN to cadherin-α-catenin fusion proteins. L cells were stably transfected with cadherin or the cadherin-α-catenin fusion proteins. These molecules were immunoprecipitated with antibodies against the GFP tag from a lysate of each transfectant, and the precipitates were analyzed to detect EPLIN by Western blotting. (*C*) L cells stably expressing GFP-tagged cadherin (*Upper*) or cadherin fusion proteins (*Lower*) indicated in *A* were double-stained for the GFP tag and F-actin. (Scale bar: 10 μm.)

β-catenin, α-catenin, and EPLIN, but not with those incubated with β-catenin and α-catenin only. GST beads incubated with β-catenin, α-catenin, and EPLIN were also negative (Fig. 4*F*). Close-up view of the positive beads displayed filamentous actins associated with their surfaces (Fig. 4*G*). These observations, supporting the recent observation that the cadherin–catenin complex alone is not able to interact with F-actin (20), demonstrates that EPLIN was indeed a direct linker between the cadherin–catenin complex and F-actin.

**The Cadherin–EPLIN Association Is Sufficient for Generating Actin-Coupling Adhesions.** Cadherins require α-catenin for their function as adhesion molecules. We tested whether EPLIN fusion to cadherin can replace the need for α-catenin as a partner. When cadherin-deficient L cells were transfected with exogenous cadherins, they restored adhesive cell–cell contacts that recruited F-actin (31). Although this activity of cadherin is lost when the β-catenin-binding region (CBR) has been deleted (Fig. 5*A*), a fusion construct between the CBR-deleted cadherin and α-catenin exhibits the normal ability to induce cadherin-based adhesions (13). Deletion of the VH3-C region of α-catenin from this fusion protein, however, again causes abrogation of the adhesion activity. Because our present results suggested that the function of α-catenin is elicited via its interaction with EPLIN, we examined whether those cadherin–α-catenin fusion proteins interacted with EPLIN or not. Immunoprecipitation experiments using L cells transfected with cDNAs for those proteins showed that EPLIN was coprecipitated not only with the full-length cadherin [Cad(FL)] but also with the cadherin-α-catenin fusion protein [Cad-αcat(FL)], but not with the CBR-deleted cadherin [Cad CBR(−)] or with the fusion protein from which the VH3-C region of α-catenin had been deleted [Cad-αcat (1–643); Fig. 5 *A* and *B*]. These results are consistent with the view that the α-catenin–EPLIN interaction is essential for this catenin to work for cell–cell adhesion.

Next, we examined whether EPLIN could be substituted for α-catenin in the fusion constructs in restoring AJ formation in L cells. Full-length or deleted EPLIN constructs were fused to the CBR-deleted cadherin (Fig. 5*A*), and the resultant fusion proteins were expressed in L cells. These fusion proteins linearly accumulated along cell–cell contacts, recruiting F-actin to the same sites, unless the C-terminal domain of EPLIN had been deleted (Fig. 5*C*). The profiles of the junctional accumulation of these constructs were similar to those of the full-length cadherin or its fusion protein with α-catenin (Fig. 5*C*). These results suggest that EPLIN was sufficient for conferring the AJ-organizing function on cadherin and that the C-terminal actin-binding domain was required for this activity and for recruiting F-actin in L cells.

## Discussion

We provided cellular and biochemical evidence that EPLIN binds α-catenin and is thus recruited into the cadherin–catenin complex, forming a novel cadherin–β-catenin–α-catenin–EPLIN complex. Our *in vitro* results also showed that the cadherin–catenin complex was able to combine with F-actin, but only when EPLIN was present. This observation is consistent with the results of recent reports showing that the cadherin–β-catenin–α-catenin complex cannot bind F-actin (20, 21), despite the known ability of α-catenin to interact with F-actin (14). These reports also suggested that α-catenin interacted with F-actin only as a free homodimer by competing with the Arp2/3 complex, leading to the proposal that the role of α-catenin would be to modulate actin polymerization (3, 32). However, our present findings provide an additional role of α-catenin. By binding to EPLIN, α-catenin functions as a component of the machinery to link cadherin to F-actin. We should therefore emphasize here that the classic view that the cadherin–catenin complex physically associates with actin filaments, which has recently been questioned (22), is likely not wrong, in light of our present results.

Without EPLIN, the actin bundles organized into the adhesion belts were lost, strongly suggesting that EPLIN is required for the maintenance of these actin fibers. EPLIN was earlier shown to have the ability to inhibit actin filament depolymerization and cross-link actin filaments in bundles and to suppress branching nucleation of actin filaments by the Arp2/3 complex, resulting in the formation of stable actin filaments (23). This ability of EPLIN, together with our findings, suggests that EPLIN acts not only in linking the cadherin–catenin complex to actin bundles, but also in actively stabilizing these bundles. We found that EPLIN was also localized along the apically located actin bundles in R2/7 cells lacking $\alpha$-catenin and that loss of EPLIN caused a disappearance of these bundles. These findings suggest that EPLIN can bind and stabilize apical actin bundles even in the absence of $\alpha$-catenin. However, it is likely that EPLIN normally controls the dynamics of actin fibers at the AJ by associating with the cadherin–catenin complex. However, despite the reported actin-stabilizing ability of EPLIN, depletion of this protein did not cause the entire disruption of actin networks in cells. The observation that EPLIN depletion did not ubiquitously affect actin polymerization implies the presence of a mechanism for EPLIN to control restricted populations of actin fibers. EPLIN was initially identified as one of the molecules whose transcription was down-regulated in certain cancer cells (25, 33). In such cells, the cadherin-mediated cell adhesion might also have been affected, causing alterations in their invasive behavior.

Importantly, upon EPLIN removal, the adhesion belts were converted into a zigzag form, at which radial actin fibers terminated. This type of junction is frequently seen in the early phases of epithelial contact formation or in fibroblasts (17, 18). These observations suggest that, whereas EPLIN is required for the association between cadherin and F-actin to form the adhesion belt, it is not required for the interaction between cadherin and radial actin fibers. It is therefore likely that there are other molecules to mediate the interaction of the cadherin–catenin complex with F-actin. As $\alpha$-catenin is, in fact, known to interact with multiple actin-binding proteins (27), we think it is likely that $\alpha$-catenin may use different partners to connect cadherins to F-actin under different physiological situations or cell types.

We previously showed that $\alpha$-catenin interacted with vinculin via the VH2 domain and that this domain was indispensable for restoring the apical adhesion belts in $\alpha$-catenin-deficient R2/7 cells; furthermore, the expression of a fusion construct of $\alpha$-catenin and vinculin was sufficient in inducing their adhesion belts (12). We, however, found that RNAi-mediated removal of vinculin from R2/7 cells expressing exogenous $\alpha$-catenin had no effect on their junctional organization, as long as EPLIN was expressed (unpublished observation). Thus, in the natural situation, EPLIN seems to play a dominant role in apical junction organization, although we do not exclude the possibility that vinculin might be required for AJ organization under specific cellular conditions or in certain cell types, as its role in Myosin VI-dependent process of junction formation has been reported (34). Irrespective of how vinculin is involved, we should stress that the VH2 domain is required for the formation of the ring-type adhesion belts characteristic of epithelial cells (12), although this domain was not essential for fibroblastic AJ formation (13). The VH2 domain is known to bind formin-1, and perturbation of their interaction also inhibits AJ formation in keratinocytes (27). It is thus likely that proteins associated with the different domains of $\alpha$-catenin cooperate for organization of the epithelial adhesion belts. To uncover the exact mechanisms of how the VH2 domain and the VH3-C region-associated EPLIN work together is therefore an important future subject.

## Materials and Methods

**Plasmid Construction and Protein Expression.** cDNAs for mouse EPLIN$\alpha/\beta$ were obtained from the RIKEN FANTOM cDNA database. Full-length or deletion constructs for each gene were amplified by standard PCR methods and subcloned into pCA-sal-Flag vector or pCA-sal-EGFP-IRES-hygro vector (35). For construction of EPLIN deletion series, amino acids 227–593 (EPLINdN) or 1–285 (EPLINdC) of EPLIN$\alpha$ were amplified. For EPLINdLIM, amino acids 1–226 and 286–593 fragments of EPLIN$\alpha$ were fused by inserting a Gly-Ser linker (BamHI site) between them. For the construction of cadherin-fusion molecules, amino acids 1–761 of chick N-cadherin [Cad CBR(−)] were fused with the EPLIN or $\alpha$-catenin deletion constructs. All constructs were sequenced for confirmation. Stealth siRNAs specific for each gene and for control siRNAs were obtained from Invitrogen. Sequences for human EPLIN and $\alpha$E-catenin were 5′-UUAUAGAGGUUUCUGAGAGGCGUGG-3′ and 5′-UCUCCAACACAGUCAUGCCACGUUU-3′, respectively. Recombinant human $\alpha$E-catenin, mouse E-cadherin-cytoplasmic region, $\beta$-catenin, and EPLIN$\alpha$ were expressed as N-terminus-cleavable or noncleavable GST-fusion proteins by using pGEX-6P or pGEX-2 vectors (GE Healthcare). Proteins were expressed in *Escherichia coli* and purified with Glutathione Sepharose beads (GE Healthcare) (SI Fig. 7). For removal of the GST tag, recombinant proteins were incubated with PreScission proteases (GE Healthcare) at 4°C for 24 h. Then the proteins were further purified and concentrated by using Microcon (Millipore).

**Cell Culture and Transfection.** MDCK, DLD-1, R2/7 (12), and L cells were cultured in a 1:1 mixture of DMEM and Ham's F-12 supplemented with 10% FCS. Cells were transfected by using Lipofectamine 2000 (Invitrogen). For siRNA transfection, 1 nM Stealth siRNAs was introduced into the cells by using Lipofectamine RNAiMAX (Invitrogen), according to the manufacturer's protocol. More than 90% of the targeted proteins were removed in each culture for all of the protein species studied here at 3–4 days after siRNA treatment (SI Fig. 8). For isolating stable cDNA transfectants, cells were selected by exposure to 250 $\mu$g/ml hygromycin B (Invitrogen). Mixtures of heterogeneous hygromycin-resistant clones were used for analysis to avoid clonal variations in the phenotypes. Latrunculin A treatment was performed at 4 days after the treatment with siRNA. The cells were fixed 30 min after adding 1 $\mu$M latrunculin A (Calbiochem) to the medium.

**Immunofluorescence Staining.** Immunofluorescence staining of cells was done as described (36). Images were recorded with a laser scanning confocal microscope (LSM510) mounted on an inverted microscope (Axiovert 200M) equipped with Plan-Apochromat ×63/1.40 NA objectives (Zeiss). All images were processed with Photoshop software (Adobe Systems).

**Immunochemical and Biochemical Assays.** For immunoprecipitation, DLD-1 cells were lysed in a lysis buffer [50 mM Tris·HCl, pH 7.5, containing 150 mM NaCl, 1% Nonidet P-40, 0.25% sodium deoxycolate, 1 mM EDTA, 10% glycerol, and a protease inhibitor mixture (GE Healthcare)]. The lysates were precleared with Protein G–Sepharose 4FF beads (GE Healthcare), incubated with specific antibodies or preimmune serum at 4°C for 2 h, followed by Protein G–Sepharose beads for 2 h. After the incubation, the beads were washed four times in W-Buffer (50 mM Tris·HCl, pH 7.5, containing 150 mM NaCl, 10% glycerol, and 1% Nonidet P-40) and subsequently suspended in Laemmli sample buffer. For *in vitro* binding assays of purified proteins, glutathione-Sepharose beads coated with 1 $\mu$M GST-tagged proteins were incubated at 4°C for 2 h with 0.5 $\mu$M GST-tag-removed proteins in 250 $\mu$l of the W-Buffer supplemented with 0.1 mg/ml BSA. After incubation, the beads were washed four times in the W-Buffer. For F-actin pull-down experiments, glutathione-Sepharose beads coated with 1 $\mu$M GST-tagged proteins were sequentially incubated at 4°C each for 1 h with 1 $\mu$M GST-tag-removed $\beta$-catenin, $\alpha$-catenin, and EPLIN$\alpha$ in 250 $\mu$l of the W-Buffer supplemented with 0.1 mg/ml BSA. After each of the incubations, the supernatants were removed, and the beads were washed four times. After the final wash, the beads were suspended in 250 $\mu$l of F-Buffer (the W-Buffer containing 0.2 mM ATP, 2 mM $MgCl_2$, 0.2 mM $CaCl_2$, and 50 $\mu$g/ml BSA) and incubated at 4°C for 2 h with 4 $\mu$g of preformed actin filaments (Cytoskeleton). Then, the beads were washed four times in the F-Buffer by centrifuging them at 3,500 × *g* for 5 min and subsequently suspended in the Laemmli sample buffer or incubated with Alexa Fluor-488 conjugated phalloidin for 10 min. Western blotting was performed as described (37), and blot signals were detected with ECL-Plus (GE Healthcare).

**Antibodies.** Polyclonal antibodies against EPLIN were raised by injection of a rabbit with GST-tagged full-length mouse EPLIN$\alpha$. The antibodies were affinity-purified by using the immunogen. The preimmune serum was collected from the same rabbit before injection of the immunogen. The follow-

ing primary antibodies were also used: rabbit polyclonal antibodies against $\alpha$-catenin (Sigma) and ZO-1 (Invitrogen); mouse mAbs against EPLIN, E-cadherin, actin (Ab-5, BD Biosciences), $\alpha$-tubulin (DM1A, Sigma), Flag-tag (M2, Sigma), GFP (7.1 + 11.1, Roche); and rat mAb against E-cadherin (ECCD-2) (38). F-actin was visualized by using Alexa Fluor 488-conjugated phalloidin (Invitrogen).

**ACKNOWLEDGMENTS.** We thank Shigenobu Yonemura, Testuhisa Otani, and other members of our laboratory for discussion and comments. This work was supported by a grant from Grants-in-Aid for Specially Promoted Research of the Ministry of Education, Science, Sports, and Culture of Japan (to M.T.) and a grant-in-aid for scientific research from the Japan Society for the Promotion of Science for Junior Scientists (to K.A.).

1. Mege RM, Gavard J, Lambert M (2006) *Curr Opin Cell Biol* 18:541–548.
2. Lecuit T (2005) *Trends Cell Biol* 15:34–42.
3. Pokutta S, Weis WI (2007) *Annu Rev Cell Dev Biol* 23:237–261.
4. Hildebrand JD (2005) *J Cell Sci* 118:5191–5203.
5. Haigo SL, Hildebrand JD, Harland RM, Wallingford JB (2003) *Curr Biol* 13:2125–2137.
6. Dawes-Hoang RE, Parmar KM, Christiansen AE, Phelps CB, Brand AH, Wieschaus EF (2005) *Development (Cambridge, UK)* 132:4165–4178.
7. Blankenship JT, Backovic ST, Sanny JS, Weitz O, Zallen JA (2006) *Dev Cell* 11:459–470.
8. Bertet C, Sulak L, Lecuit T (2004) *Nature* 429:667–671.
9. Otani T, Ichii T, Aono S, Takeichi M (2006) *J Cell Biol* 175:135–146.
10. Hirano S, Kimoto N, Shimoyama Y, Hirohashi S, Takeichi M (1992) *Cell* 70:293–301.
11. Watabe M, Nagafuchi A, Tsukita S, Takeichi M (1994) *J Cell Biol* 127:247–256.
12. Watabe-Uchida M, Uchida N, Imamura Y, Nagafuchi A, Fujimoto K, Uemura T, Vermeulen S, van Roy F, Adamson ED, Takeichi M (1998) *J Cell Biol* 142:847–857.
13. Imamura Y, Itoh M, Maeno Y, Tsukita S, Nagafuchi A (1999) *J Cell Biol* 144:1311–1322.
14. Rimm DL, Koslov ER, Kebriaei P, Cianci CD, Morrow JS (1995) *Proc Natl Acad Sci USA* 92:8813–8817.
15. Sako Y, Nagafuchi A, Tsukita S, Takeichi M, Kusumi A (1998) *J Cell Biol* 140:1227–1240.
16. Lambert M, Choquet D, Mege RM (2002) *J Cell Biol* 157:469–479.
17. Yonemura S, Itoh M, Nagafuchi A, Tsukita S (1995) *J Cell Sci* 108: 127–142.
18. Vaezi A, Bauer C, Vasioukhin V, Fuchs E (2002) *Dev Cell* 3:367–381.
19. Kametani Y, Takeichi M (2007) *Nat Cell Biol* 9:92–98.
20. Yamada S, Pokutta S, Drees F, Weis WI, Nelson WJ (2005) *Cell* 123:889–901.
21. Drees F, Pokutta S, Yamada S, Nelson WJ, Weis WI (2005) *Cell* 123:903–915.
22. Gates J, Peifer M (2005) *Cell* 123:769–772.
23. Maul RS, Song Y, Amann KJ, Gerbin SC, Pollard TD, Chang DD (2003) *J Cell Biol* 160:399–407.
24. Chen S, Maul RS, Kim HR, Chang DD (2000) *Gene* 248:69–76.
25. Maul RS, Chang DD (1999) *Oncogene* 18:7838–7841.
26. Dexter DL, Spremulli EN, Fligiel Z, Barbosa JA, Vogel R, VanVoorhees A, Calabresi P (1981) *Am J Med* 71:949–956.
27. Kobielak A, Fuchs E (2004) *Nat Rev Mol Cell Biol* 5:614–625.
28. Provost E, Rimm DL (1999) *Curr Opin Cell Biol* 11:567–572.
29. Vasioukhin V, Bauer C, Yin M, Fuchs E (2000) *Cell* 100:209–219.
30. Wulf E, Deboben A, Bautz FA, Faulstich H, Wieland T (1979) *Proc Natl Acad Sci USA* 76:4498–4502.
31. Nagafuchi A, Shirayoshi Y, Okazaki K, Yasuda K, Takeichi M (1987) *Nature* 329:341–343.
32. Weis WI, Nelson WJ (2006) *J Biol Chem* 281:35593–35597.
33. Chang DD, Park NH, Denny CT, Nelson SF, Pe M (1998) *Oncogene* 16:1921–1930.
34. Maddugoda MP, Crampton MS, Shewan AM, Yap AS (2007) *J Cell Biol* 178:529–540.
35. Ichii T, Takeichi M (2007) *Genes Cells* 12:827–839.
36. Abe K, Chisaka O, Van Roy F, Takeichi M (2004) *Nat Neurosci* 7:357–363.
37. Abe K, Takeichi M (2007) *Neuron* 53:387–397.
38. Shirayoshi Y, Nose A, Iwasaki K, Takeichi M (1986) *Cell Struct Funct* 11:245–252.